arXiv:cond-mat/0510697v1 [cond-mat.mtrl-sci] 26 Oct 2005

Magneto-optics in pure and defective $Ga_{1-x}Mn_xAs$ from first–principles

S. Picozzi,[1] A. Continenza[1], M. Kim[2,3] and A. J. Freeman[2]

[1]*INFM-CNR, CASTI Regional Lab. and Dip. Fisica, Università degli Studi dell'Aquila, 67100 Coppito (L'Aquila), Italy*

[2]*Department of Physics and Astronomy, Northwestern University, Evanston,IL 60208 (U.S.A.)*

[3]*Department of Physics, Seoul National University, Korea*

Abstract

The magneto-optical properties of $Ga_{1-x}Mn_xAs$ including their most common defects were investigated with precise first–principles density-functional FLAPW calculations in order to: *i*) elucidate the origin of the features in the Kerr spectra in terms of the underlying electronic structure; *ii*) perform an accurate comparison with experiments; and *iii*) understand the role of the Mn concentration and occupied sites in shaping the spectra. In the substitutional case, our results show that most of the features have an interband origin and are only slightly affected by Drude–like contributions, even at low photon energies. While not strongly affected by the Mn concentration for the intermediately diluted range ($x \sim 10\%$), the Kerr factor shows a marked minimum (up to 1.5^o) occurring at a photon energy of ~ 0.5 eV. For interstitial Mn, the calculated results bear a striking resemblance to the experimental spectra, pointing to the comparison between simulated and experimental Kerr angles as a valid tool to distinguish different defects in the diluted magnetic semiconductors framework.

PACS numbers: 75.50.Pp,78.20.Ls

The magneto-optical (MO) Kerr effect is known since 1877 when Kerr[1] observed that linearly polarized light reflected from a magnetic surface becomes elliptically polarized with the major axis rotated with respect to the incident light. The Kerr effect, as well as other closely related spectroscopic effects, such as the Faraday effect and magnetic circular dichroism, can be traced back to the different interaction of left- and right- circularly polarized light with a magnetized solid. MO effects are therefore powerful experimental probes that play a relevant role in clarifying the electronic structure of ferromagnets and providing detailed information on the influence of broken time-reversal symmetry in itinerant quasi-particle electron states[2].

Within the fascinating field of semiconductor spintronics[3], transition metal doped semiconductors, due to their unusual magnetic and electronic properties, have been the focus of intense research in the last few years. The early prototype material is undoubtefully $Ga_{1-x}Mn_xAs$[4], a dilute magnetic semiconductor (DMS) with $x < 10\%$ and a Curie temperature < 150 K, for which its ferromagnetism is generally explained in terms of a hole-carrier-mediated exchange mechanism. Although the electronic and magnetic properties of $Ga_{1-x}Mn_xAs$ have been extensively studied, to our knowledge *ab–initio* calculations for the MO properties of $Ga_{1-x}Mn_xAs$ have not been reported. The focus of this work is therefore to perform an accurate comparison with extensively performed experiments[5, 6, 7], in order to: *(i)* assess the validity of the first principles electronic structure theory and *(ii)* to explain the main features in the MO spectra of GaMnAs on the basis of its electronic structure.

In our approach based on density functional theory (DFT), the Kohn-Sham equations are solved self-consistently using the highly accurate full–potential linearized augmented plane wave (FLAPW) [8] method. Spin-orbit coupling (SOC), essential to describe MO effects, neglected in the self–consistent cycle, is included as a second variational step [9] in the evaluation of the optical conductivity tensor, σ_{ij}.[10] For metals (or half-metals, such as GaMnAs), the components of the optical conductivity tensor are given by a sum of interband and intraband contributions. The interband transitions are obtained according to the Kubo formalism within linear response theory through momentum matrix elements Π_{ij}:[11],

$$\sigma_{\alpha\beta}(\omega) \;=\; \frac{i}{\omega V}\int \frac{d\mathbf{k}}{(2\pi)^3}\sum_{i,j}\left(\frac{\Pi^{\alpha}_{ji}\Pi^{\beta}_{ij}}{\omega+i\tau-\epsilon_{ij}}-\frac{\Pi^{\alpha}_{ij}\Pi^{\beta}_{ji}}{\omega+i\tau+\epsilon_{ij}}\right), \qquad \alpha,\beta=x,y,z \qquad (1)$$

where ω is the photon energy, ϵ_{ij} are differences between eigenvalues and τ is the interband relaxation time. The intraband contribution is added to the diagonal components of the

conductivity tensor with a phenomenological Drude expression: $\sigma = \frac{\omega_p^2}{4\pi(1-i\omega\tau_D)}$ where the plasma frequency is given by: $\omega_p = \frac{4\pi e^2}{m^2 V}\sum_{i\mathbf{k}}\delta(\epsilon_{i\mathbf{k}} - E_F)|\Pi_{ii}^{\alpha}|^2$ (E_F is the Fermi energy and τ_D is the intraband relaxation time).

Here, we only consider the Kerr effect in the so-called *polar geometry*, in which the incident wave vector and magnetization are perpendicular to the surface. In this case, the Kerr rotation angle $\theta_k(\omega)$ and its ellipticity $\varepsilon_k(\omega)$ can be obtained from the conductivity tensor as follows[2]:

$$\theta_k(\omega) + i\varepsilon_k(\omega) \;=\; -\frac{\sigma_{xy}(\omega)}{\sigma_{xx}(\omega)\sqrt{1 + i(4\pi/\omega)\sigma_{xx}(\omega)}} \tag{2}$$

In order to investigate the effect of Mn concentration on the MO properties, we considered different unit cells (each containing a single Mn impurity and with the GaAs experimental lattice constant, a = 10.69 a.u.) – a bcc- and an fcc-crystal for a 6.25 % and a 12.5 % Mn concentration, respectively. We used a basis set of plane waves with wave vector up to K_{max}=3.5 a.u. and an angular momentum expansion up to l_{max} = 8 for both the potential and charge density. The muffin-tin radius, R_{MT}, for Mn, Ga and As was chosen equal to 2.1, 2.3, and 2.3 a.u., respectively. The Brillouin zone (BZ) was sampled using a (4,4,4) Monkhorst-Pack[12] cubic shell, whereas the optical conductivity was computed using up to 216 special **k**-points. In order to investigate the effects of the most common defects on the MO properties, we also considered 32-atom cells with *i*) an interstitial Mn, *ii*) an As-antisite, *i.e.* a substitutional Mn located at the origin along with an As-antisite located at $(a/2, a/2, 0)$, and *iii*) an interstitial-substitutional dimer coupled antiferromagnetically. Although, according to DFT predictions, the most energetically favorable site is the substitutional one, the possibility for some Mn to occupy the interstitial sites and that As antisites are formed during severely–out–of–equilibrium growth cannot be ruled out, as several experiments appear to show.[13]

We first focus on the most diluted systems (x = 6.25%) with Mn in the substitutional position; these can presumably be well compared with available experiments[6, 7]. Figure 1 (a) shows the real part of the complex Kerr angle with different values of the broadening (bold and dashed lines). The remarkable thing is that, for a small broadening of $\hbar/\tau$ = 0.1 eV, the Kerr rotation can reach values of more than 1.5^o: this unexpectedly high Kerr rotation may open the way to magneto-optical applications using DMS. However, it is also evident that the maximum value of the Kerr rotation is markedly dependent on the smearing

value used: already with a larger broadening ($\hbar/\tau = 0.3$ eV), the Kerr rotation shows a value of the order of 0.5 degrees, typically observed in $3d$ ferromagnets[2]. Incidentally, we also note that our calculated spectrum using the smaller broadening is in remarkable agreement with model calculations[14] based on a Kohn-Luttinger Hamiltonian and a kinetic exchange interaction – not only the spectral shape, but also the energy position of the peaks is in good coincidence.

The peculiar shape of the Kerr rotation, with the strong resonance at $\sim$ 0.5 eV and several other features at higher energies, can be fully explained in terms of the numerator ($\omega\sigma_{xy}$) and denominator ($\omega D = \omega\sigma_{xx}(\omega)\sqrt{1 + i(4\pi/\omega)\sigma_{xx}(\omega)}$ in Eq.2, therefore separating the MO and optical contributions, respectively (see Fig.1 (d)). The deep resonance at $\sim$ 0.5 eV can be ascribed to the minimum of the denominator, whereas the other peaks follow the numerator trend, in turn due to the interplay of the SOC and exchange splitting. The strong resonance at low energies has therefore an "optical" origin, whereas the high energy part is instead due to MO effects. In order to investigate whether the presence of the strong resonance - given its relatively low energy - is due to an intraband or interband contribution, the Kerr rotation without the Drude contribution is also shown (see bold vs thin line) in Fig.1 (b). As expected, the exact position of the peak is affected by the Drude contribution (or, equivalently, by the plasma frequency) but the deep resonance is kept and is therefore seen to have mainly an interband origin.

In order to further investigate the MO properties and, in particular, the effect of the Mn concentration, we show in Fig.2 (c) the calculated Kerr rotation and ellipticity, for the 6.25 % and 12.5 % case. The overall trend as a function of frequency is quite similar for the two concentrations, confirming that in this intermediate diluted regime the concentration of magnetic impurities does not strongly affect the electronic structure – consistent with previous reports.[15] In particular, the principal features for relevant energies < 2 eV are present in both concentration cases – the peaks only differ in their energy positions. This rather weak dependence on concentration was already noted from the experiment by Lang *et al.* [7] that measured a Kerr rotation that is comparable in size upon more-than-doubling the concentration (*i.e.* Kerr spectra were measured for $x = 0.014$ and 0.03), although some of the features as a function of energy varied significatively with the concentration.

Moreover, it is of interest to compare our results for the substitutional case (see first column in Fig.2) with available experimental spectra, measured in the very diluted limit ($x \sim$

1-3%)[7] as well as for a concentration similar to this work ($x \sim 6\%$)[6]. Although the order of magnitude is consistent, there are some discrepancies between theory and experiment. In particular, the experimental Kerr rotation is always negative, whereas theoretical spectra show some crossing with the zero y axis. However, the energy position of the minimum at $\sim$ 1.5-2 eV and of the maximum at $\sim$ 2.5-3 eV is reproduced in our spectra.

As for the Kerr ellipticity, there are some similarities between theory and experiment regarding the crossing of the zero axis as well as the order of magnitude, but also some severe discrepancies (especially in the low energy range). There might be several reasons for this disagreement, among which we mention: *i*) the poor description of features in the DFT electronic structure related to excited or correlated states[16] and *ii*) the fact that the calculations are done at zero temperature. Indeed, most of the measurements have been done at higher temperatures, where the magnetization is expected to be smaller, therefore giving rise to a smaller Kerr angle. As a confirmation of that, we recall that experiments by Kojima *et al.*[6] were performed at 77 K with a Curie temperature of 110 K (and, therefore, the measurements were done at a temperature not much lower than T_C); on the other hand, experiments by Lang *et al.* were performed at 1.8 K with a Curie temperature of 60 K and the samples clearly show a saturated magnetization. As a result, the Kerr signal in the latter case is higher than in the former case; moreover, consistent with this temperature dependence, our results - which ideally reproduce the situation at 0 K or, at least, in the condition of saturated magnetization - predict a rather high value of the Kerr angle.

The disorder that might be present in the samples is another reason that could explain the discrepancy between theory and experiment. Therefore, in order to investigate the effects of the most common defects on the MO properties, we also show in Fig. 2 the calculated Kerr angles for (b) the interstitial Mn and (c) substitutional Mn along with an As-antisite. Clearly, different Mn positions or the presence of antisites significatively change the spectra, pointing to a possible use of the MO Kerr effect to distinguish substitutional and interstitial Mn, antisites, etc. In particular, it is immediately evident that there is a very good agreement as far as the Kerr rotation and ellipticity are concerned for the interstitial case — as is evident both with small and large broadenings (see solid and dashed line in Fig.2) used to better reproduce the experiments by Lang[7] and Kojima[6], respectively. This might be explained as follows: most of the samples[6] were annealed and it is well known that annealing brings interstitials to the surface. Therefore, the Kerr technique, which mostly probes the surface

samples, sees an enhanced contribution from the interstitials. As far as the ellipticity only is concerned, we note that a generally satisfying agreement is reached also for the As-antisite. We do not provide plots for the interstitial-substitutional Mn dimers, since the agreement is rather poor, as expected. In fact, this is compatible with the idea that the samples in Ref.[6] were annealed at 280^o C, and so the dimers - possibly formed during the low–temperature growth - are expected to be split and to no longer exist in such an appreciable density as to give a strong contribution to the Kerr spectra.

Finally, we point out that our DFT-FLAPW simulations for hexagonal MnAs, which are in good agreement with previously published spectra[17] and therefore not reported here, show a much larger (on the order of 0.5 degrees over the whole energy range) Kerr rotation and ellipticity — and strikingly different from experiments for $Ga_{1-x}Mn_xAs$. Therefore, the comparison between theory and experiment confirms that the Kerr signal is not due to precipitates in the samples and suggests that this kind of simulations is a valid means to reveal competing phases that can frequently occur during DMS growth[18].

In summary, accurate FLAPW calculations within density functional theory and the Kubo formalism were performed focusing on the optical and magneto–optical properties of GaMnAs. The maximum Kerr angle, occurring at a photon energy of <0.5 eV, can reach high values ($> 1.5\ ^o$) and is mainly due to an optical rather than a magneto-optical origin. In the intermediate diluted regime ($x \sim 10\%$), the Kerr spectra do not depend dramatically on concentration and are mostly due to interband, rather than intraband, contributions. For Mn in the substitutional position, the comparison with experiments for the Kerr rotation and ellipticity shows some disagreement. On the other hand, the spectra are quite well reproduced for interstitial Mn, suggesting that the Kerr effect might be used to distinguish the MO response of substitutional rather than interstitial Mn. However, the role that the somewhat inaccurate treatment of correlation or many–body effects within a single-particle DFT description of the GaMnAs electronic structure might have in shaping the Kerr spectra has still to be investigated.

Work at Northwestern University supported by the National Science Foundation Grant No. DMR-0244711/002.

---

[1] J. Kerr, Philos. Mag. **3**, 231 (1877).

[2] W. Reim and J. Schoenes, in *Ferromagnetic Materials*, E. P. Wohlfarth and K.H.J. Buschow (Eds.), North-Holand, Amsterdam (1988), Vol. 5, p. 133; V. N. Antonov, A. N. Yaresko, A. Ya. Perlov, V. V. Nemoschalenko, P. M. Oppeneer and H. Eschrig, Low Temp. Phys. **25**, 387 (1999); H. Ebert, Rep. Prog. Phys. **59**, 1665 (1996) and references therein.

[3] S. A. Wolf, D. D. Awschalom, R. A. Buhrman, R. A. Daughton, S. von Molnar, M. L. Roukes, A. Y. Chtchelkanova, and D. M. Treger, Science **294**, 1488 (2001).

[4] T. Dietl, H. Ohno, F. Matsukura, J. Cibert and D. Ferrand, Science **287**, 1019 (2000).

[5] H. Munekata, slides from
http://solidstate.physics.sunysb.edu/lees2002/speakers/munekata/LEES02_final1_150dpi.pdf

[6] E. Kojima, R. Shimano, Y. Hashimoto, S. Katsumoto, Y. Iye, and M. Kuwata-Gonokami, Phys. Rev. B **68**, 193203 (2003).

[7] R. Lang, A. Winter, H. Pascher, H. Krenn, X. Liu and J. K. Furdyna, Phys. Rev. B **72**, 024430 (2005).

[8] E. Wimmer, H. Krakauer, M. Weinert and A. J. Freeman, Phys. Rev.B **24**, 864 (1981).

[9] A. H. Mac Donald, W. E. Pickett and D. D. Koelling, J. Phys. C **13**, 2675 (1980).

[10] M. Kim, A. J. Freeman and R. Wu, Phys. Rev.B **59**, 9432 (1999).

[11] H. Ebert, Rep. Prog. Phys. **59**, 1665 (1996)

[12] H.J.Monkhorst and J.D.Pack, Phys. Rev. B **13**, 5188 (1976).

[13] K. W. Edmonds, N. R. S. Farley, R. P. Campion, C. T. Foxon, B. L. Gallagher, T. K. Johal, G. van der Laan, M. MacKenzie, J. N. Chapman, and E. Arenholz Appl. Phys. Lett. **84**, 4065 (2004).

[14] E. M. Hankiewicz, T, Jungwirth, T. Dietl, C. Timm and J. Sinova, Phys. Rev. B **70**, 245211 (2004) .

[15] Yu-Jun Zhao, W. T. Geng, K. T. Park, and A. J. Freeman Phys. Rev. B **64**, 035207 (2001)

[16] Calculations according to an LSDA+U approach (see V.I. Anisimov, F. Aryasetiawan, and A.I. Lichtenstein, J. Phys.: Condens. Matter **9**, 767 (1997).) for treating correlated Mn d states are planned.

[17] P. Ravindran, A. Delin, P. James, B. Johansson, J. M. Wills, R. Ahuja, and O. Eriksson Phys. Rev. B **59**, 15680 (1999).

[18] See for example J.-S. Kang, G. Kim, S. C. Wi, S. S. Lee, S. Choi, Sunglae Cho, S. W. Han, K. H. Kim, H. J. Song, H. J. Shin, A. Sekiyama, S. Kasai, S. Suga, and B. I. Min, Phys. Rev.

FIG. 1: (a) Calculated Kerr rotation for Mn in the substitutional site for different smearings — of 0.1 eV (dashed line) and 0.3 eV (bold solid line) — as a function of energy. Circles denote values from model calculations.[14] (b) Comparison between total (interband + intraband) contributions (bold solid line) and interband only (thin solid). (c) Effect of Mn concentration: $x = 6.25\%$ (bold solid line) and $x = 12.5\%$ (dot-dashed line). (d) Kerr rotation broken down in numerator (*i.e.* MO part, dot-dashed line, right y-axis) and denominator (*i.e.* optical part, solid line, left y-axis), see text for details.

FIG. 2: Calculated complex Kerr angle (thin solid line) for an energy broadening of 0.3 eV: rotation (upper panels) and ellipticity (lower panels) for (a) substitutional Mn, (b) interstitial Mn and (c) substitutional Mn along with an As antisite. Experimental data are marked by symbols: circles, diamonds and squares for Refs.[6], [7] and [5], respectively. In panel (b), we also show the Kerr rotation calculated with a small broadening ($\hbar/\tau = 0.1$ eV, see dashed line).

Lett. **94**, 147202 (2004).

Fig. 1 - Picozzi et al.

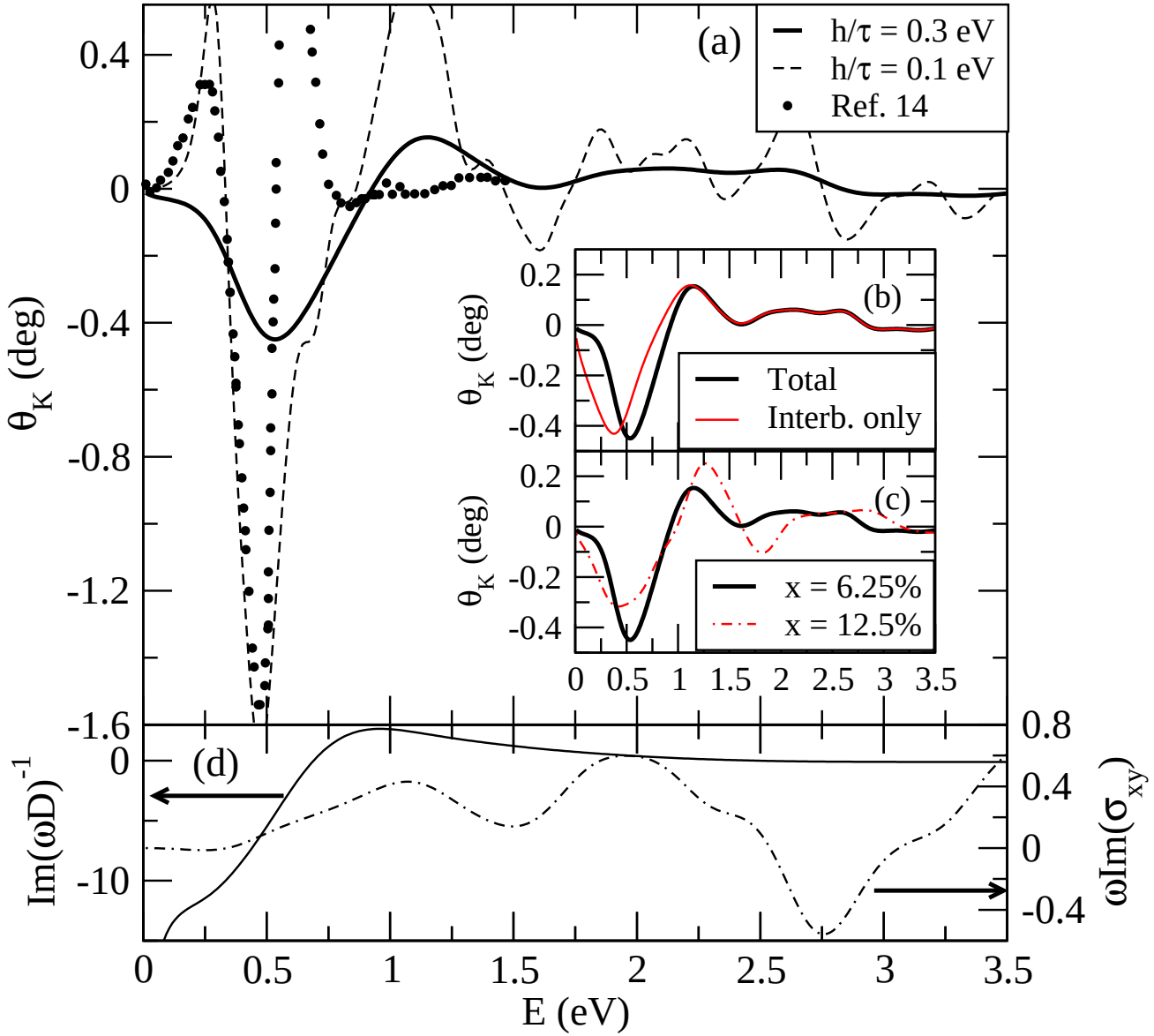

Fig. 2 - Picozzi et al.